An offline-online homogenization strategy to solve quasilinear two-scale problems at the cost of one-scale problems

Assyr Abdulle, Yun Bai, Gilles Vilmart

An offline-online homogenization strategy to solve quasilinear two-scale problems at the cost of one-scale problems

A. Abdulle[1*], Y. Bai[1], and G. Vilmart[2]

[1]*ANMC, Section de Mathématiques, École Polytechnique Fédérale de Lausanne, 1015 Lausanne, Switzerland, Assyr.Abdulle@epfl.ch, Yun.Bai@epfl.ch*

[2]*École Normale Supérieure de Cachan, Antenne de Bretagne, INRIA Rennes, IRMAR, CNRS, UEB, Campus de Ker Lann, F-35170 Bruz, France, Gilles.Vilmart@bretagne.ens-cachan.fr*

SUMMARY

Inspired by recent analyses of the finite element heterogeneous multiscale method and the reduced basis technique for nonlinear problems, we present a simple and concise finite element algorithm for the reliable and efficient resolution of elliptic or parabolic multiscale problems of nonmonotone type. Solutions of appropriate cell problems on sampling domains are selected by a greedy algorithm in an offline stage and assembled in a reduced basis (RB). This RB is then used in an online stage to solve two-scale problems at a computational cost comparable to the single-scale case. Both the offline and the online cost are independent of the smallest scale in the physical problem. The performance and accuracy of the algorithm are illustrated on 2D and 3D stationary and evolutionary nonlinear multiscale problems.

KEY WORDS: nonlinear nonmonotone problems, numerical homogenization, reduced basis method, a posteriori error estimator, finite element method

1. INTRODUCTION

The aim of the proposed algorithm is to solve multiscale quasilinear elliptic problems of the form

$$-\nabla\cdot(a^\varepsilon(x,u^\varepsilon(x))\nabla u^\varepsilon(x)) = f(x) \ \text{ in } \Omega, \qquad u^\varepsilon = 0 \ \text{ on } \partial\Omega, \tag{1}$$

or parabolic problems of the form

$$\frac{\partial u^\varepsilon(x,t)}{\partial t} - \nabla\cdot(a^\varepsilon(x,u^\varepsilon(x,t))\nabla u^\varepsilon(x,t)) = f(x,t) \ \text{ in } \Omega\times[0,T], \quad u^\varepsilon = 0 \ \text{ on } \partial\Omega\times[0,T], \tag{2}$$

where a^ε is a nonlinear tensor that oscillates rapidly in space at the scale ε, at a computational cost analogous to that of standard finite element methods (FEM) for single-scale quasilinear elliptic or parabolic problems. We recall that solving (1) or (2) by a standard FEM requires, for small ε, a very fine mesh width $h<\varepsilon$ leading to a prohibitive computational cost.

For simplicity, we assume that Ω is a polyhedral domain in $\mathbb{R}^d$, $d\le 3$, and we consider homogeneous Dirichlet boundary conditions. Here, f is a source term and the nonlinear tensors $a^\varepsilon(x,s)$ are matrices of size $d\times d$ which are assumed uniformly elliptic and bounded with respect to x, s and ε,

$$\lambda|\xi|^2 \le a^\varepsilon(x,s)\xi\cdot\xi, \quad |a^\varepsilon(x,s)\xi| \le \Lambda_1|\xi|, \quad \forall\xi\in\mathbb{R}^d, \forall s\in\mathbb{R}, \text{ a.e. } x\in\Omega, \tag{3}$$

*Correspondence to: ANMC, Section de Mathématiques, École Polytechnique Fédérale de Lausanne, 1015 Lausanne, Switzerland. Assyr.Abdulle@epfl.ch.

Contract/grant sponsor: The research of A. A. and Y. B. is partially supported by the Swiss National Foundation; contract/grant number: 200021_134716.

and Lipchitz continuous with respect to s,

$$|a^\varepsilon(x,s_1)\xi - a^\varepsilon(x,s_2)\xi| \le \Lambda_2|\xi||s_1-s_2|, \quad \forall \xi \in \mathbb{R}^d, \forall s_1,s_2 \in \mathbb{R}, \text{ a.e. } x \in \Omega, \tag{4}$$

where $\lambda, \Lambda_1, \Lambda_2 > 0$ are independent of ξ, s, s_1, s_2, x.

Standard homogenization theory for such nonlinear problems [1, 2, 3] states that u^ε converges as $\varepsilon \to 0$ (up to a subsequence) weakly in $H^1(\Omega)$[†] toward a homogenized solution u^0 which is solution of a one-scale effective problem of the same form as (1),

$$-\nabla \cdot \big(a^0(x,u^0(x))\nabla u^0(x)\big) = f(x) \text{ in } \Omega, \qquad u^0 = 0 \text{ on } \partial\Omega. \tag{5}$$

The tensor $a^0(x,s)$ in (5), called the homogenized tensor, is in general unknown and needs to be approximated numerically [4, 5]. For simplicity, we assume that the tensor a^ε (and thus also a^0) is symmetric, but we emphasize that the algorithm could be extended to non-symmetric problems.

The method, called the reduced basis finite element heterogeneous multiscale method (RB-FE-HMM) combines the finite element heterogeneous multiscale method (FE-HMM) [6, 7, 8, 9] with a reduced order model strategy, namely the reduced basis (RB) method. The RB-FE-HMM, proposed in [10, 11] for linear problems, is based on an offline-online strategy: one first computes a representative reduced basis for appropriate microscopic sampling cell problems which permits to recover the (upscaled) homogenized solution u^0. In addition, a corrector procedure permits to reconstruct the oscillatory solution u^ε from the homogenized one at a negligible overcost. Indeed, an important feature of the (RB-)FE-HMM is that its computational cost is independent of the smallness of the parameter ε because the mesh width of the domain Ω can be much larger than ε and appropriate cell problems are solved on sampling domains of size that scale with ε.

The convergence analysis of the RB-FE-HMM for nonlinear elliptic problems (1) of nonmonotone type was recently proposed in [12], with a study of the coupling of the reduced basis technique with the FE-HMM for computing the homogenized solution of quasilinear multiscale elliptic problems of nonmonotone type [7, 9].

For solving numerically one-scale quasilinear elliptic problem of the form (5), a standard approach is the a finite element method (FEM) together with a Newton method as analyzed in [13, 14]. Considering a FEM space $S_0^\ell(\Omega,\mathcal{T}_H)$ with mesh grid size H, such method approximates a solution u^H of

$$B_H(u^H;u^H,w^H) = F_H(w^H), \quad \forall w^H \in S_0^\ell(\Omega,\mathcal{T}_H), \tag{6}$$

by a sequence $u_k^H, k = 0,1,2,3,\dots$ and reads in weak form

$$\partial B_H(u_k^H;u_{k+1}^H - u_k^H, w^H) = F_H(w^H) - B_H(u_k^H;u_k^H,w^H), \quad \forall w^H \in S_0^\ell(\Omega,\mathcal{T}_H), \tag{7}$$

where $\partial B_H(z^H;v^H,w^H) := B_H(z^H;v^H,w^H) + B_H'(z^H;v^H,w^H)$. We used the notations

$$B_H(z^H;v^H,w^H) := \sum_{K\in\mathcal{T}_H}\sum_{j=1}^J \omega_{K_j} a^0(x_{K_j},z^H(x_{K_j}))v^H(x_{K_j})\nabla z^H(x_{K_j})\cdot\nabla w^H(x_{K_j}), \tag{8}$$

$$B_H'(z^H;v^H,w^H) := \sum_{K\in\mathcal{T}_H}\sum_{j=1}^J \omega_{K_j} \partial_s a^0(x_{K_j},z^H(x_{K_j})v^H(x_{K_j})\nabla z^H(x_{K_j})\cdot\nabla w^H(x_{K_j}), \tag{9}$$

and $F_H(w^H)$ is an approximation of $\int_\Omega f w^H dx$. Here, we consider the FEM space

$$S_0^\ell(\Omega,\mathcal{T}_H) = \{v^H \text{ is continuous on } \Omega,\ v^H = 0 \text{ on } \partial\Omega;\ v^H|_K \in \mathcal{R}^\ell(K),\ \forall K \in \mathcal{T}_H\},$$

where $\mathcal{T}_H$ is a shape-regular family of partition of Ω in simplicial or quadrilateral elements K of diameter H_K where we denote $H := \max_{K\in\mathcal{T}_H} H_K$ and $\mathcal{R}^\ell(K)$ is the space $\mathcal{P}^\ell(K)$ of polynomials on K of total degree at most ℓ if K is a simplicial FE, or the space $\mathcal{Q}^\ell(K)$ of polynomials on K of degree at most ℓ in each variable if K is a quadrilateral FE. For each element K of the partition

[†]We denote $H^1(\Omega)$ the Sobolev space of square integrable functions in $L^2(\Omega)$ which have square integrable derivatives.

we consider a quadrature formula $(\omega_{K_j}, x_{K_j})_{j=1,\dots,J}$ with weights ω_{K_j} and nodes x_{K_j} fulfuling the usual assumptions (see [15] in the context of linear elliptic problems).

It can be observed that the Newton method in (7), (8), (9) requires the evaluation of $a^0(x_{K_j}, s)$ for all quadratures nodes x_{K_j} of all FEM elements $K \in \mathcal{T}_H$ and all nonlinear parameter $s = u_k^H(x_{K_j})$ of the iterate functions of the Newton evaluated at the quadrature nodes. Thus for the FE-HMM, one needs to compute $a^0(x_{K_j}, s)$ (by a micro FEM) at each quadrature node for each iteration of the Newton method. As in addition the degrees of freedom (DOF) of the micro FE space have to increase simultaneously with the DOF of the macro FE space $S_0^\ell(\Omega, \mathcal{T}_H)$ for optimal convergence [9, 6], a numerical homogenization method such as the FE-HMM can become expensive especially for high-dimensional nonlinear problems.

This paper is organized as follows. In Section 2, we present an offline procedure based on the reduced basis (RB) technique which permits to precompute the homogenized tensor a^0. Then, we describe in Section 3 how an online procedure, with a computational cost analogous to that of solving a one scale problem, permits to compute the homogenized solution u^0. In Section 4, we describe a reconstruction procedure for approximating the oscillatory solution u^ε at a negligible overcost. In Section 5, the performance of the algorithm is illustrated on a 2D time dependent test problem and a 3D brake rotor problem.

2. OFFLINE PROCEDURE

This section describes the offline stage of the RB-FE-HMM which permits to precompute the nonlinear homogenized tensor a^0 that is needed in the online stage to compute the homogenized solution u^0 itself.

The idea of the algorithm is to recover the microscopic oscillations by considering suitable sampling domains $K_{\delta_j} \subset \Omega$ defined as follows. For each macro element $K \in \mathcal{T}_H$ and each quadrature point $x_{K_j} \in K$, $j = 1, \dots, J$, we define the sampling domains $K_{\delta_j} = x_{K_j} + \delta(-1/2, 1/2)^d$, $(\delta \geq \varepsilon)$, where $Y = (-1/2, 1/2)^d$. We observe that each sampling domain K_{δ_j} is in correspondence with Y through the affine transformation

$$y \in Y \mapsto G_{x_{K_j}}(y) = x_{K_j} + \delta y \in K_{\delta_j} \tag{10}$$

For each sampling domain K_{δ_j}, we introduce the corresponding oscillatory tensor defined as

$$a_{x_{K_j},s}(y) := a^\varepsilon(G_{x_{K_j}}(y), s). \tag{11}$$

Notice that if the tensor a^ε is locally periodic, i.e. has the form $a^\varepsilon(x, s) = a(x, x/\varepsilon, s)$ with periodicity with respect to the second argument x/ε, then we shall consider instead

$$a_{x_{K_j},s}(y) := a(x_{K_j}, G_{x_{K_j}}(y), s),$$

and if in addition the oscillatory period ε is known, we shall take $\delta = \varepsilon$ for the size of the sampling domains K_{δ_j}. We next assume that an affine representation of the tensors $a_{x_{K_j},s}$ is available, i.e. we have the following decomposition:

$$a_{x,s}(y) = \sum_{p=1}^{P} \Theta_p(x, s) a_p(y), \ \forall y \in Y. \tag{12}$$

Notice that if the above affine representation of the tensor is not available, then the empirical interpolation method (EIM) can be used to derive such affine representation (see [16]). For all the point x in Ω and all parameter s, consider the linear cell problem: find $\hat{\psi}^{i,s}_{\mathcal{N},x} \in S^q(Y, \mathcal{N})$ such that

$$b(\hat{\psi}^{i,s}_{\mathcal{N},x}, \hat{z}_\mathcal{N}) = -\int_Y a_{x,s}(y)\mathbf{e}_i \cdot \nabla \hat{z}_\mathcal{N}(y) dy \ \ \forall \hat{z}_\mathcal{N} \in S^q(Y, \mathcal{N}), \tag{13}$$

where we use the notation

$$b(\hat{v}, \hat{z}) := \int_Y a_{x,s}(y) \nabla \hat{v}(y) \cdot \nabla \hat{z}(y) dy \ \ \forall \hat{v}, \hat{z} \in W^1_{per}(Y),$$

and $\mathbf{e}_i, i = 1, \dots, d$ denotes the canonical basis of $\mathbb{R}^d$. Considering the Sobolev space $W^1_{per}(Y)$ of periodic functions[‡] in $H^1(Y)$, we consider a micro FE space $S^q(Y, \mathcal{N}) \subset W^1_{per}(Y)$ with simplicial or quadrilateral FEs and piecewise polynomial of degree q on the domain $Y = (-1/2, 1/2)^d$ equipped with a conformal and shape regular family of triangulation denoted $\mathcal{T}_{\hat{h}}$, and $\mathcal{N} = \mathcal{O}(\hat{h}^{-d})$ denotes the number of degrees of freedom (DOF) of this FE space.

The idea of the offline procedure is to avoid the computation of the solutions of the cell problem (13) for all quadrature nodes x_{K_j} and all parameter $s = u^H_k(x_{K_j})$ lying in a compact subspace $\mathcal{D}$ of $\Omega \times \mathbb{R}$. Instead we compute a small set of representative basis functions $\hat{\xi}_{l,\mathcal{N}}, l = 1, \dots, N$ that span the RB space

$$S_N(Y) := span\{\hat{\xi}_{1,\mathcal{N}}, \dots, \hat{\xi}_{N,\mathcal{N}}\}. \tag{14}$$

The above *hatmap* notation is used to recall that these functions are defined over the reference domain Y. These RB functions are computed using a greedy procedure that selects representative cell problems and relies on a suitable a posteriori error estimator described below. Given a parameter (x, s, i) we consider the solutions $\hat{\xi}^{i,s}_{\mathcal{N},T_\delta}, \hat{\xi}^{i,s}_{l,T_\delta}$ of (13) in $S^q(Y, \mathcal{N})$ and $S_l(Y)$, respectively (i.e. with test functions $\hat{z}_\mathcal{N}$ in $S^q(Y, \mathcal{N})$ and $S_l(Y)$, respectively) and define the residual

$$\hat{e}^{i,s}_{l,T_\delta} \quad = \quad \hat{\xi}^{i,s}_{l,T_\delta} - \hat{\xi}^{i,s}_{\mathcal{N},T_\delta}. \tag{15}$$

Then by the Riesz theorem, there exists a unique $\bar{e}^i_{l,T_\delta} \in S^q(Y, \mathcal{N})$ such that

$$b(\hat{e}^{i,s}_{l,T_\delta}, \hat{z}_\mathcal{N}) = (\bar{e}^{i,s}_{l,T_\delta}, \hat{z}_\mathcal{N})_\mathcal{W}, \ \forall \hat{z}_\mathcal{N} \in S^q(Y, \mathcal{N}), \tag{16}$$

where we consider the scalar product $(u, v)_\mathcal{W} = \int_Y \nabla u(y) \cdot \nabla v(y) dy$ on the Hilbert space $W^1_{per}(Y)$ and the corresponding norm $\|v\|_\mathcal{W} = \sqrt{(v, v)_\mathcal{W}}$.

A posteriori error estimator. The a posteriori error estimator for the parameter (x_τ, s, i) is then defined as

$$\Delta^{i,s}_{l,T_\delta} := \frac{\|\bar{e}^{i,s}_{l,T_\delta}\|_\mathcal{W} + \|\partial_s \bar{e}^{i,s}_{l,T_\delta}\|_\mathcal{W}}{\sqrt{\lambda_{LB}}}, \tag{17}$$

where λ_{LB} with $\lambda_{LB} \leq \lambda$ is an approximation of the coercivity constant λ defined in (3) (see e.g. [17]). The residual $\partial_s \bar{e}^{i,s}_{l,T_\delta}$ in (17) is defined by differentiating with respect to s the FE problem (16). This a posteriori error estimator is designed to guaranty not only the convergence of the RB-FE-HMM, but also the Newton method convergence and the uniqueness of the numerical solution, as analyzed in [14] using the a posteriori error estimates for $i, j = 1, \dots, d$, $l = 1, \dots, N$,

$$C_1 \Delta^i_{l,T_\delta} \leq \|\hat{e}^{i,s}_{l,T_\delta}\|_\mathcal{W} + \|\partial_s \hat{e}^{i,s}_{l,T_\delta}\|_\mathcal{W} \leq C_2 \Delta^i_{l,T_\delta} \tag{18}$$

where C_1, C_2 depend on $\lambda, \Lambda_1, \Lambda_2, \lambda_{LB}$ in (3), (4). The above estimator can be computed as follows. In view of (16), considering the decomposition $\hat{\xi}^{i,s}_{l-1,T_\delta} = \sum_{j=1}^{l-1} \alpha_j(s) \hat{\xi}_{j,\mathcal{N}}$ in the RB space S_{l-1}, we compute following the implementation in [17, Sect. 4.4]

$$\bar{e}^{i,s}_{l,T_\delta} = \sum_{p=1}^{P} \Theta_p(x, s) \left(\sum_{j=1}^{l-1} \alpha_j(s) L_{p,j} - M_{p,i} \right) \tag{19}$$

where $L_{p,j}, M_{p,i} \in S^q(Y, \mathcal{N}), p = 1, \dots, P, i = 1, \dots, d, j = 1, \dots, N$ are obtained by solving the FE projection problems

$$(L_{p,j}, \hat{z}_\mathcal{N})_\mathcal{W} = \int_Y a_p(y) \nabla \hat{\xi}_{j,\mathcal{N}}(y) \cdot \nabla \hat{z}_\mathcal{N}(y) dy, \quad (M_{p,i}, \hat{z}_\mathcal{N})_\mathcal{W} = \int_Y a_p(y) \nabla \mathbf{e}_i \cdot \nabla \hat{z}_\mathcal{N}(y) dy, \ \forall \hat{z}_\mathcal{N} \in S^q(Y, \mathcal{N}).$$

Notice that the functions $L_{p,j}, M_{p,i}$ are independent of the parameter x, s and thus computed only once.

[‡]Notice that $H^1_0(Y)$ could also be considered for a coupling with Dirichlet boundary conditions and sampling domain size $\delta > \varepsilon$, see the review [5].

Remark 2.1
The FE approximation of $\partial_s \bar{e}^{i,s}_{l,T_\delta}$ in (17) (that could be obtained by solving the appropriate FEM problem) are simply calculated by using the finite difference approximation

$$\partial_s \bar{e}^{i,s}_{l,T_\delta} \approx \frac{\bar{e}^{i,s+\sqrt{eps}}_{l,T_\delta} - \bar{e}^{i,s}_{l,T_\delta}}{\sqrt{eps}},$$

where eps is the machine precision. This can be done by computing $\bar{e}^{i,s}_{l,T_\delta}$ in (19) with parameters s and $s+\sqrt{eps}$, respectively. Thus, the cost of computing $\bar{e}^{i,s}_{l,T_\delta}$ and $\partial_s \bar{e}^{i,s}_{l,T_\delta}$ is twice the cost of evaluating $\bar{e}^{i,s}_{l,T_\delta}$ alone.

RB construction by the Greedy algorithm We now describe the construction procedure of the RB in (14) based on the a posteriori error estimator (17).

A first step is the guess of the range of nonlinear parameters $s = u^H(x_{K_j})$ involved in the nonlinear tensor $a(x,s)$. This is done using the following empirical algorithm motivated by the Voigt-Reiss inequality [18, Chapter 1.6],

$$\Big(\int_Y a_{x,s}(y)^{-1} dy\Big)^{-1} \leq a^0(x,s) \leq \int_Y a_{x,s}(y) dy, \tag{20}$$

for parameters x, s, and where $a^0(x,s)$ is the homogenized tensor. We then apply the following procedure to derive the training set $\mathcal{D}$, a compact of $\Omega \times \mathbb{R}$.

Algorithm 2.2 (Construction of the training set)

1. Using a standard one-scale FEM method, solve (5) where the homogenized tensor $a^0(x,s)$ is replaced alternatively with the tensors of the left and right-hand sides of (20).
2. Set a maximum range $(u^{0,low}, u^{0,up})$ by taking the minimum and maximum values of the two solutions using theses easy to evaluate tensors.
3. Define the training set as $\mathcal{D} = \Omega_\delta \times [u^{0,low} - \alpha, u^{0,up} + \alpha]$ where Ω_δ is a compact subset of Ω such that for any $x \in \Omega_\delta$ the corresponding sampling domain centered at x is inscribed in Ω, and the range of parameter s is enlarged by $\pm\alpha$ (a safety factor of about 10%).

Based on the training set $\mathcal{D}$, we may now state the Greedy algorithm inspired by the usual RB methodology (see [19, 20]).

Algorithm 2.3 (Greedy procedure)
Given the maximum basis number N_{RB} and an error tolerance tol_{RB}:

1. Choose randomly (by a Monte Carlo method) N_{train} parameters $(x_n, s_n) \in \mathcal{D}, d = 1, \ldots, N_{train}$. Define the "training set" $\Xi_{RB} = (x_n, s_n, \eta_n); 1 \leq \eta_n \leq d, 1 \leq n \leq N_{train}\}$.
2. Select randomly $(x_1, s_1, \eta_1) \in \Xi_{RB}$ and compute $\hat{\xi}^{\eta_1,s_1}_{\mathcal{N},T_{\delta_1}} \in S^q(Y,\mathcal{N})$, the solution of (13) with the selected parameters $x = x_1, s = s_1, i = \eta_1$. Set $l = 1$ and define $\hat{\xi}_{1,\mathcal{N}}(y) = \frac{\hat{\xi}^{\eta_1,s_1}_{\mathcal{N},T_{\delta_1}}(y)}{\|\hat{\xi}^{\eta_1,s_1}_{\mathcal{N},T_{\delta_1}}\|_{\mathcal{W}}}$.
3. For $l = 2, \ldots, N_{RB}$
   a. Compute for each $(x,s,\eta) \in \Xi_{RB}$ the residual $\Delta^{\eta,s}_{l-1,T_\delta}$ defined in (17) and compute

$$(x_l, s_l, \eta_l) = argmax_{(x,s,\eta)\in\Xi_{RB}} \Delta^{\eta,s}_{l-1,T_\delta}.$$

   If [§] $\max_{(T_\delta,s,\eta)\in\Xi_{RB}} (\Delta^{\eta,s}_{l-1,T_\delta})^2 > tol_{RB}$ then go to b., otherwise the algorithm ends.

[§]Notice that the error of the outputs of interest scale like the square of the error of the cell functions, see (23) in Remark 3.1.

b. Compute $\hat{\xi}^{\eta_l,s_l}_{\mathcal{N},T_{\delta_l}}$ the solution of (13) in $S^q(Y,\mathcal{N})$ corresponding to (x_l,s_l,η_l) selected in a., and define the next RB function $\hat{\xi}_{l,\mathcal{N}}$ using the orthogonalization procedure

$$\hat{\xi}_{l,\mathcal{N}}(y) := \frac{R_l(y)}{\|R_l\|_{\mathcal{W}}}, \quad \text{where} \quad R_l(y) := \hat{\xi}^{\eta_l,s_l}_{\mathcal{N},T_{\delta_l}}(y) - \sum_{m=1}^{l-1} (\hat{\xi}^{\eta_l,s_l}_{\mathcal{N},T_{\delta_l}}, \hat{\xi}_{m,\mathcal{N}})_{\mathcal{W}} \hat{\xi}_{m,\mathcal{N}}.$$

Set $l = l+1$ and go back to a.

What is next needed for the online procedure is the $N \times N$ stiffness matrices A_p and the length N vectors $F_{p,i}$, with $p = 1,\dots,P, i = 1,\dots,d$, defined as

$$(A_p)_{mn} = \int_Y a_p(y) \nabla \hat{\xi}_{n,\mathcal{N}}(y) \cdot \nabla \hat{\xi}_{m,\mathcal{N}}(y) dy, \qquad F_{p,i} = \int_Y a_p(y) \mathbf{e}_i \cdot \nabla \hat{\xi}_{m,\mathcal{N}}(y) dy.$$

We shall also need the matrix of averages

$$(G_p)_{mn} = \int_Y a_p(y) \mathbf{e}_m \cdot \mathbf{e}_n dy = \int_Y (a_p(y))_{mn} dy.$$

The above integrals on Y can be computed using a sufficiently accurate quadrature formula on the micro mesh $\mathcal{T}_{\hat{h}}$ of the micro FEM space $S^q(Y,\mathcal{N})$.

3. ONLINE PROCEDURE

The online version of the RB-FE-HMM is identical to a standard FEM with numerical quadrature applied to a one-scale problem (5) using a Newton method. The only difference is that one has to approximate the homogenized tensor $a^0(x_{K_j},s)$ for a given quadrature node x_{K_j} and a nonlinear parameter s. We explain how this can be performed at a negligible overcost using the output of the offline procedure.

In the case of a locally periodic tensor a^ε, the homogenized tensor coefficients given by the homogenization theory [2] can be written as

$$(a^0(x,s))_{mn} = \int_Y a_{x_{K_j},s}(y) \left(\hat{\psi}^{m,s}_x(y) + \mathbf{e}_m \right) \cdot \mathbf{e}_n dy, \quad m,n = 1,\dots,d,$$

where $\hat{\psi}^{m,s}_x \in W^1_{per}(Y)$ is the solution of the cell problem (13) with test functions in $W^1_{per}(Y)$. Analogously, we define the numerical homogenized tensor a^0_N as

$$(a^0_N(x,s))_{mn} = \int_Y a_{x,s}(y) \left(\nabla \hat{\psi}^{m,s}_{N,x}(y) + \mathbf{e}_m \right) \cdot \mathbf{e}_n dy, \quad m,n = 1,\dots,d, \tag{21}$$

where $\hat{\psi}^{m,s}_{N,x} \in S_N(Y),\ m = 1,\dots,d$ is the solution of (13) in the RB space $S_N(Y)$, i.e. with test functions in $S_N(Y)$. This function can be decomposed in the RB space $S_N(Y)$ as

$$\hat{\psi}^{m,s}_{N,x}(y) = \sum_{j=1}^N \alpha_j^{(x,s,m)} \hat{\xi}_{j,\mathcal{N}}, \tag{22}$$

where $\boldsymbol{\alpha}^{(x,s,m)} = (\alpha_1^{(x,s,m)},\dots,\alpha_N^{(x,s,m)})^T$ is the vector of coordinates in this basis.

Remark 3.1
Notice that the a posteriori error estimates (18) also control the accuracy of the quantity of interest $a^0_N(x,s)$ in (21). Precisely, we have (see [12])

$$|(a^0_{\mathcal{N}}(x,s))_{mn} - (a^0_N(x,s))_{mn}| \le \Delta^{m,s}_{l,T_\delta} \Delta^{n,s}_{l,T_\delta}, \quad m,n = 1,\dots,d, \tag{23}$$

where the tensor $a^0_{\mathcal{N}}(x,s)$ is defined similarly to (21) but using the functions $\hat{\psi}^{m,s}_{\mathcal{N},x} \in S^q(Y,\mathcal{N})$, solutions of the cell problem (13) with test functions in $S^q(Y,\mathcal{N})$.

Elliptic case. Inspired by (21) and the decomposition (22), we are now in position to state the algorithm for the online procedure to compute the homogenized solution u^0 of the multiscale quasilinear problem (1).

Algorithm 3.2 (Online algorithm for elliptic problems (1))
Given an initial guess $u_0^H \in S_0^\ell(\Omega, \mathcal{T}_H)$, compute the Newton method sequence $u_k^H, k = 1, 2, 3, \ldots$ defined in (7), where B_H and ∂B_H are defined similarly to (8), (9), with the unknown homogenized tensor $a^0(x, s)$ replaced by the numerical tensor $a_N^0(x, s)$ and computed as

$$(a_N^0(x,s))_{mn} = \sum_{p=1}^{P} \Theta_q(x,s)\big(\boldsymbol{\alpha}^{(x,s,m)} \cdot F_{p,n} + (G_p)_{mn}\big), \quad m, n = 1, \ldots, d,$$

where the vectors $\boldsymbol{\alpha}^{(x,s,i)} \in \mathbb{R}^N$ with $i = 1, \ldots, d$ are obtained by solving the $N \times N$ linear system

$$\left(\sum_{p=1}^{P} \Theta_p(x,s) A_p\right) \boldsymbol{\alpha}^{(x,s,i)} = -\sum_{p=1}^{P} \Theta_p(x,s) F_{p,i}. \tag{24}$$

The derivative $\partial_s a_N^0(x, s)$ of the numerical tensor involved in ∂B_H can be computed using a finite difference formula (analogously to $\partial_s \bar{e}_{l,T_\delta}^{i,s}$ in Remark 2.1).

It is proved in [9, 12] that under suitable smoothness assumptions, the Newton method in the online algorithm 3.2 is well defined and converges for sufficiently fine mesh parameters H, h to the approximation u^H of u^0. This numerical solution u^H is uniquely defined. We observe that the a posteriori estimator (17) involving the derivative of the Riesz projection of the residual (15) is instrumental for establishing the convergence of the Newton method.

Parabolic case. We next explain the extension of the algorithm for solving parabolic problems (2). First, we note that for quasilinear parabolic problems, the effective tensor can be computed by solving time-independent (quasilinear elliptic) problems. Second, we observe that Algorithm 2.2 can be applied to obtain the training set by solving standard parabolic FE problems using the bounds in (20). Finally, we can use the Algorithm 2.3 for the Greedy procedure.

Notice that various time integrators can be used in the online stage of RB-FE-HMM, see e.g. [21] in the context of linear multiscale parabolic problems. Here, we use the linearized backward Euler (see [22] for details) and consider a constant time stepsize. Its advantage over the standard backward Euler scheme is that it permits to avoid Newton iterations.

Algorithm 3.3 (Online algorithm for parabolic problems (2))
Given the time step Δt and $u_0^H \in S_0^\ell(\Omega, \mathcal{T}_H)$ associated to the initial condition, compute u_n^H, $n = 1, 2, 3, \ldots$ the solution at time $t = n\Delta t$, of the linear system

$$\int_\Omega \frac{u_n^H - u_{n-1}^H}{\Delta t} v^H dx + B_H(u_{n-1}^H; u_n^H, v^H) = F_H(v^H), \ \forall v^H \in S_0^\ell(\Omega, \mathcal{T}_H), \tag{25}$$

where the form B_H is computed identically as is Algorithm 3.2.

4. CONSTRUCTION OF A CORRECTOR

The online algorithm 3.2 permits to approximate the homogenized solution u^0 of the multiscale problem (1) as $\varepsilon \to 0$. To reconstruct the oscillatory solution u^ε of (1) for a fixed value of ε, and in turn obtaining an approximation of u^ε in the energy norm (i.e. $u_{corr}^\varepsilon \simeq u^0 + \varepsilon u^1$), a suitable corrector procedure is needed [23, 18] and can be obtained as follows. Consider the linear multiscale problem

$$-\nabla \cdot \big(a^\varepsilon(x, u^0) \nabla v^\varepsilon(x)\big) = f(x) \ \text{ in } \Omega, \qquad v^\varepsilon = 0 \ \text{ on } \partial\Omega,$$

where compared to (1), the tensor is evaluated at u^0 instead of u^ε. It is shown in [2, Sect. 3.4.2] that a corrector u_{corr} for the above linear problem is also a corrector for the solution u^ε of the nonlinear problem (1). This permits to define the following numerical corrector for the approximation of u^ε similarly to the linear case.

Nonlinear corrector Given a quadrature point $x_{K_j} \in K \in \mathcal{T}_H$, we consider the inverse map $\widetilde{G}_{x_{K_j}} := G_{x_{K_j}}^{-1} : T_{\delta_j} \to Y$ where $G_{x_{K_j}}$ is defined in (10). We next extend this map periodically on the macro element K by setting $\widetilde{G}_{x_{K_j}}(x + \delta \boldsymbol{k}) = \widetilde{G}_{x_{K_j}}(x)$ for all $\boldsymbol{k} \in \mathbb{Z}^d, x \in T_{\delta_j}$. We next define for all $x \in K$,

$$u_{corr}^{H,\varepsilon}(x) := u^H(x) + \varepsilon \hat{\psi}_{N,x_0}^{m,s}\big(\widetilde{G}_{x_{K_j}}(x)\big) \simeq u^\varepsilon(x),$$

where $u^H \in S_0^\ell(\Omega, \mathcal{T}_H)$ is the output of the online algorithm 3.2 and the functions $\hat{\psi}_{N,x_0}^{m,s} \in S_N(Y)$ can be evaluated using the RB decomposition (22) with the RB produced by the Greedy algorithm 2.3. Notice that the coefficients $\alpha_j^{(x,s,m)}$ in (22) are already computed (24) and need not to be recomputed.

5. NUMERICAL EXPERIMENTS

We illustrate the performances of the proposed implementation of RB-FE-HMM on various elliptic and parabolic multiscale problems in 2D and 3D. We compare the algorithm with the standard nonlinear FE-HMM code [9] designed without the reduced basis technique, and based on the implementation in [24] in the context of linear problems. We consider here (non-parallel[¶]) implementations made in Matlab on a desktop computer.

5.1. A 2D time dependent problem

We consider a time dependent test problem of the form (2). We choose an example where a reference solution can be easily computed to check the accuracy of the method, and we take the affine tensor with diagonal entries

$$\begin{aligned} a^\varepsilon(x,s)_{11} &= (x_1^2 + 0.2) + (x_2 \sin(s\pi) + 2)(\sin(2\pi \frac{x_1}{\varepsilon}) + 2), \\ a^\varepsilon(x,s)_{22} &= (\frac{1}{s+1} e^{x_2} + 0.05) + (x_1 x_2 + 1)(\sin(2\pi \frac{x_2}{\varepsilon}) + 2), \end{aligned} \tag{26}$$

defined on the domain $\Omega = [0,1]^2$ and we choose the boundary conditions

$$\begin{aligned} u^\varepsilon(x,t) &= g_D(x), \quad \text{on } \{x_1 = 0\} \cup \{x_1 = 1\}, \\ n \cdot (a^\varepsilon(x, u^\varepsilon(x,t)) \nabla u^\varepsilon(x,t)) &= g_N(x), \quad \text{on } \{x_2 = 0\} \cup \{x_2 = 1\}. \end{aligned} \tag{27}$$

It follows from the homogenization theory [18], that the homogenized tensor corresponding to (26) is diagonal with entries given by the harmonic averages

$$a_{ii}^0 = \Big(\int_Y a(x,y,s)^{-1} dy \Big)^{-1}, \ i = 1, 2.$$

We set $f(x) = 50 e^{(x_1 - 0.2)^2 + (x_2 - 0.3)^2}$, $g_D = 1$ and $g_N = 0$. We choose $u^\varepsilon(x,0) = 1$ as the initial condition, and we consider the time interval $[0,T] = [0, 0.5]$.

We apply the offline stage as described in Sect. 2 and obtain the RB with 8 functions. The offline settings and output are presented in Table I.

In this computation, we set the time step $\Delta t = 0.001$ (so that the corresponding $\mathcal{O}(\Delta t)$ error is negligible compared to the spatial discretization). A reference solution u^{ref} is computed by using the standard FEM with piecewise linear FEs applied to the homogenized problem with tensor a^0, with a mesh grid 257×257 and the linearized backward Euler scheme as time integrator. We can see from Fig. 1 that we obtain the usual convergence rates for the FEM applied to parabolic problems. Indeed, $\|u^H - u^{ref}\|_{L^2([0,T];H^1(\Omega))}$ decreases with rate $\mathcal{O}(H)$ and $\|u^H - u^{ref}\|_{L^\infty([0,T];L^2(\Omega))}$ decreases with rate $\mathcal{O}(H^2)$.

We list the online CPU times in Table II for various macro meshes of the square domain Ω. We tested that the CPU time cost for the FE-HMM with $N_{MAC} = N_{MIC} = 65$ for one time step is

[¶]Notice that the linear systems (24) involving different parameters x, s are independent and can be solved in parallel.

Table I. Offline settings and output for the time dependent problem (2) with boundary conditions (27).

Parameter space	$[0,1]^2 \times [0.9, 3.93]$
Train set size	4400
Mesh	1500×1500
tol_{RB}	1e-10
RB Basis number	8

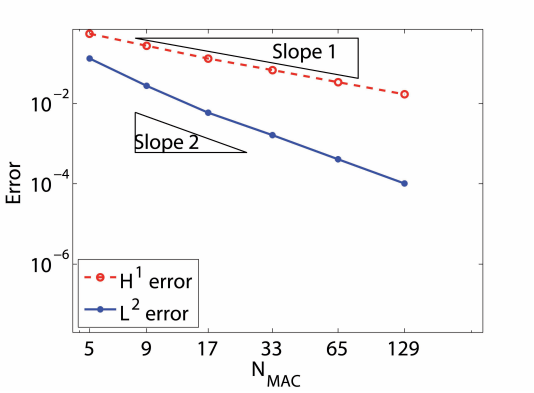

Figure 1. Time dependent problem (2), (27) with $T = 0.5$. We plot the errors $\|u^H - u^{ref}\|_{L^\infty([0,T];L^2(\Omega))}$ and $\|u^H - u^{ref}\|_{L^2([0,T];H^1(\Omega))}$ versus $N_{MAC} = 1/H$ for the RB-FE-HMM.

280s. As we have $T/\Delta t = 500$ time steps, the total CPU time for the FE-HMM without reduced basis would be about 39 hours. In contrast, the RB-FE-HMM CPU time is only 446s, i.e. 300 times less. The total CPU time of the RB-FE-HMM (including the offline procedure) is only 1.3% of the FE-HMM cost.

Table II. Online CPU times for the parabolic test problem (2), (27), $T = 0.5, \Delta t = 0.001$.

Macro mesh	5×5	9×9	17×17	33×33	65×65
Online CPU time	14.87	17.53	19.49	26.46	445.93

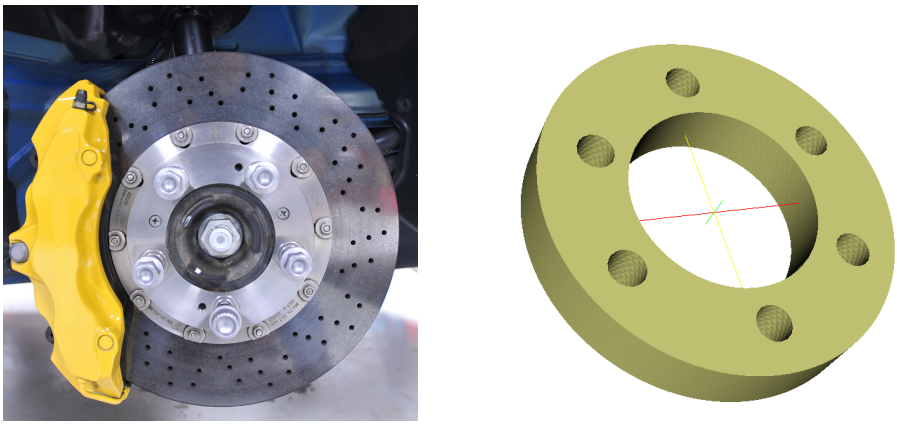

Figure 2. Left picture: example of a rotor break system in a car. Right picture: the geometry of the brake rotor part considered as the computational domain Ω.

5.2. Heat transfer in a 3D rotor

To illustrate the performances of the RB-FE-HMM, we consider in this section a simplified model in 3D inspired from [25] of a car brake rotor in a stationary regime (see left picture of Fig. 2).

We focus on the heat propagation in a part of the rotor as the break system is activated. The geometry of this part is represented in Fig. 2 (right picture). Its external and internal radius are given respectively by $R = 15$cm and $r = 8$cm and its thickness is 5cm. We assume that the material has a composite structure with a microscopic characteristic length ε. We consider a nonlinear heat propagation modeled by problem (1) with heat source $f = 0$ where $u^\varepsilon(x)$ denotes the temperature (in Kelvin degrees) as a function of x in the 3D computational domain. The nonlinear multiscale conductivity tensor is assumed diagonal with entries given by

$$\begin{aligned} a^\varepsilon_{11}(x,s) &= \alpha(s)\big(\cos(4\pi\frac{x_3}{\varepsilon})+2\big)+\beta(x)\big(\sin(2\pi\frac{x_1}{\varepsilon})+2\big),\\ a^\varepsilon_{22}(x,s) &= \alpha(s)\big(\cos(4\pi\frac{x_1}{\varepsilon})+2\big)+\beta(x)\big(\sin(2\pi\frac{x_2}{\varepsilon})+2\big),\\ a^\varepsilon_{33}(x,s) &= \alpha(s)\big(\cos(4\pi\frac{x_2}{\varepsilon})+2\big)+\beta(x)\big(\sin(2\pi\frac{x_3}{\varepsilon})+2\big), \end{aligned}$$

where $\alpha(s) = 0.01\big(e^{-(s-300)^2}+0.5\big)$, $\beta(x) = \big(0.001(x_1^2+x_2^2+x_3^2)\big)^{1/2}+0.005$. Our aim here is to show the capability of our nonlinear algorithm on a realistic 3D geometry and we therefore choose to model the microstructure by ad-hoc oscillatory tensors. We note that for realistic composite materials these conductivity tensors could be obtained via imaging techniques. We next describe the boundary conditions that are considered in the model. The external circular boundary surface (diameter R) of the considered rotor part is attached to a brake plate (see left picture in Fig. 2). It permits to slow down and stop the disk rotation by the friction due to the brake pads pushing against this brake plate (yellow part). The heat flux arising from the braking is modeled by a Neumann boundary condition on this external cylindrical boundary

$$-\nabla\cdot\big(a^\varepsilon(x,u^\varepsilon(x))\nabla u^\varepsilon(x)\big)\cdot n = g_B \tag{28}$$

where n is the external unit vector normal to the boundary and we set the surface power $g_B = 75 Wm^{-2}$. The six small holes in the computational domain (see Fig. 2) as well as the main hole in the center are normally filled with screws or other components (not considered here) and we choose for simplicity homogeneous Neumann boundary conditions at these interfaces (we thus use (28) with g_B replaced by zero). The rest of the boundary is in contact with air at temperature $u^{ext} = 293.15\,K$. The corresponding convective heat transfer is modeled by a Robin boundary condition and we use (28) with g_B replaced by $-\alpha(u^\varepsilon(x)-u^{ext})$ and set $\alpha = 10 Wm^{-2}K^{-1}$.

We apply the RB-FE-HMM to this 3D problem and we collect the offline parameters and in Table IV. For the online stage, we consider a macro mesh of the computational domain Ω with about 90000 tetrahedra generated by Cubit13.2 [26]. The CPU time for the online stage of the

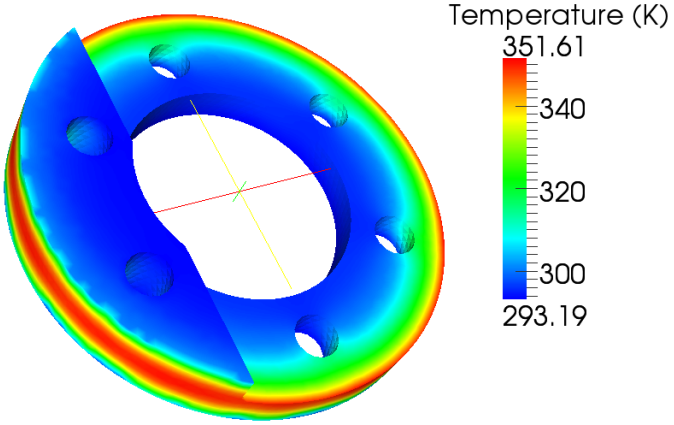

Figure 3. RB-FE-HMM macro solution u^H of the 3D brake rotor elliptic problem.

Table III. RB offline pre-process for the 3D rotor problem. $DOF = 17804$.

Tensor type	$\min \bar{u}_H^0$	$\max \bar{u}_H^0$
$< a(x,y;s) >_Y$	293.2	348.7
$< a(x,y;s)^{-1} >_Y^{-1}$	293.2	353.7

Table IV. Offline parameters and output for the 3D rotor problem.

Parameter space	$\Omega \times [288, 360]$
Training set size	4000
Number of tetrahedra	29478000
tol_{RB}	1e-8
RB Basis number	6

nonlinear elliptic RB-FE-HMM is 96.4s for 6 Newton iterations. In Fig. 3, we plot the computed temperature distribution on the rotor (a cut parallel to the top surface is displayed to see the internal heat distribution). As we can see, the range of the computed temperature is $[293.85, 349.2]$ which lies in our training set based on the data in Table III.

We finally consider the parabolic model of the form (2) where we use the same boundary conditions as above and we consider the initial temperature $u^\varepsilon(x,0) = u^{ext} = 293.15\,K$ and

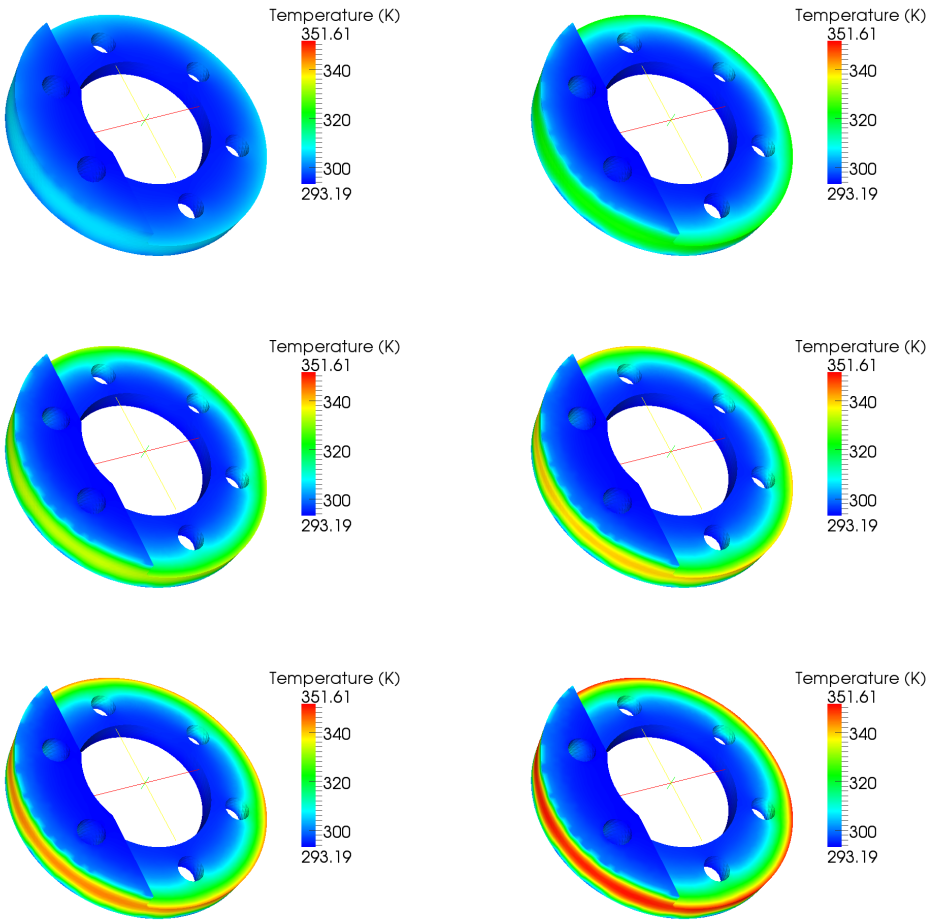

Figure 4. RB-FE-HMM macro solution of the 3D brake rotor parabolic model at times $t = 0.6, 2.4, 4.2, 6.0, 7.8, 50$ (respectively from left to right and top to bottom).

consider the time interval $[0, T] = [0, 50]$. The RB produced by the offline procedure of the elliptic problem can be reused for this time evolutionary problem because the range of temperature in Table III remains valid. The CPU computational time for the parabolic online stage is $8\,s$ per time step, using a constant time step $\Delta t = 0.2$. We plot in Figure 4 the RB-FE-HMM solutions obtained by the parabolic online procedure. We observe that the heat propagates from the exterior to the interior of the rotor and approaches the steady solution (Figure 3).

6. CONCLUSION

We have presented an efficient implementation of the RB-FE-HMM algorithm for the resolution of elliptic or parabolic nonlinear multiscale problems at the cost of single-scale nonlinear problems. This proposed algorithm combines a numerical homogenization strategy (the FE-HMM) with a model reduction strategy (the RB method). The accuracy of the model reduction strategy and the outputs of interest are controlled by an appropriate a posteriori error estimator for nonlinear problems. A remarkable feature of the offline-online strategy is that the computational cost of the method is independent of the smallness of the oscillatory parameter ε and the oscillatory solution u^ε can be reconstructed from the homogenized one u^0 with negligible overhead. The efficiency of the proposed algorithm has been illustrated on two and three dimensional time dependent nonlinear problems on a non-trivial computational domain.

REFERENCES

1. Artola M, Duvaut G. Un résultat d'homogénéisation pour une classe de problèmes de diffusion non linéaires stationnaires. *Ann. Fac. Sci. Toulouse Math.* 1982; **4**(5):1–28.
2. Boccardo L, Murat F. Homogénéisation de problèmes quasi-linéaires. *Publ. IRMA, Lille* 1981; **3**(7):13–51.
3. Fusco N, Moscariello G. On the homogenization of quasilinear divergence structure operators. *Ann. Mat. Pura Appl.* 1987; **146**(4):1–13.
4. Fish J ((ed.)). *Multiscale methods*. Oxford University Press: Oxford, 2010. Bridging the scales in science and engineering.
5. Abdulle A, E W, Engquist B, Vanden-Eijnden E. The heterogeneous multiscale method. *Acta Numer.* 2012; **21**:1–87, doi:doi:10.1017/S0962492912000025.
6. Abdulle A. On a priori error analysis of fully discrete heterogeneous multiscale FEM. *SIAM, Multiscale Model. Simul.* 2005; **4**(2):447–459.
7. E W, Ming P, Zhang P. Analysis of the heterogeneous multiscale method for elliptic homogenization problems. *J. Amer. Math. Soc.* 2005; **18**(1):121–156.
8. Abdulle A. Analysis of a heterogeneous multiscale FEM for problems in elasticity. *Math. Models Methods Appl. Sci.* 2006; **16**(4):615–635.
9. Abdulle A, Vilmart G. Analysis of the finite element heterogeneous multiscale method for quasilinear elliptic homogenization problems. *To appear in Math. Comp.* 2012; .
10. Abdulle A, Bai Y. Reduced basis finite element heterogeneous multiscale method for high-order discretizations of elliptic homogenization problems. *J. Comput. Phys.* 2012; **231**(21):7014–7036.
11. Abdulle A, Bai Y. Adaptive reduced basis finite element heterogeneous multiscale method. *Comput. Methods Appl. Mech. Engrg.* 2013; **257**:201–220.
12. Abdulle A, Bai Y, Vilmart G. Reduced basis finite element heterogeneous multiscale method for quasilinear elliptic homogenization problems. *Submitted* 2013; .
13. J Douglas J, Dupont T. A Galerkin method for a nonlinear Dirichlet problem. *Math. Comp.* 1975; **29**(131):689–696.
14. Abdulle A, Vilmart G. A priori error estimates for finite element methods with numerical quadrature for nonmonotone nonlinear elliptic problems. *Numer. Math.* 2012; **121**(3):397–431, doi:10.1007/s00211-011-0438-4.
15. Ciarlet P, Raviart P. The combined effect of curved boundaries and numerical integration in isoparametric finite element methods. *Math. Foundation of the FEM with Applications to PDE* 1972; :409–474.
16. Barrault M, Maday Y, Nguyen N, Patera A. An 'empirical interpolation method': Application to efficient reduced-basis discretization of partial differential equations. *C. R. Acad. Sci. Paris* 2004; **Ser.I 339**:667–672.
17. Patera AT, Rozza G. *Reduced Basis Approximation and A Posteriori Error Estimation for Parametrized Partial Differential Equations*. to appear in (tentative rubric) MIT Pappalardo Graduate Monographs in Mechanical Engineering, 2007.
18. Jikov V, Kozlov S, Oleinik O. *Homogenization of differential operators and integral functionals*. Springer-Verlag: Berlin, Heidelberg, 1994.
19. Prud'homme C, Rovas DV, Veroy K, Machiels L, Maday Y, Patera AT, Turinici G. Reliable real-time solution of parametrized partial differential equations: Reduced-basis output bounds methods. *J. Fluids Eng.* 2002; **124**:70–80.
20. Rozza G, Huynh D, Patera AT. Reduced basis approximation and a posteriori error estimation for affinely parametrized elliptic coercive partial differential equations. *Arch. Comput. Methods. Eng.* 2008; **15**:229–275.
21. Abdulle A, Vilmart G. Coupling heterogeneous multiscale FEM with Runge-Kutta methods for parabolic homogenization problems: a fully discrete space-time analysis. *Math. Models Methods Appl. Sci.* 2012; **22**(6):1250 002/1–1250 002/40.

22. Nie YY, Thomée V. A lumped mass finite-element method with quadrature for a non-linear parabolic problem. *IMA Journal of Numerical Analysis* 1985; **5**:371–396.
23. Bensoussan A, Lions JL, Papanicolaou G. *Asymptotic analysis for periodic structures*. North-Holland Publishing Co.: Amsterdam, 1978.
24. Abdulle A, Nonnenmacher A. A short and versatile finite element multiscale code for homogenization problem. *Comput. Methods Appl. Mech. Engrg* 2009; **198**(37-40):2839–2859.
25. Talati F, Jalalifar S. Analysis of heat conduction in a disk brake system. *Heat Mass Transfer* 2009; **45**:1047–1059.
26. Sandia National Lab. Geometry and mesh generation toolkit, http://cubit.sandia.gov 1997-2013.